DOI: 10.1002/chem.201000635

Do Dynamic Effects Play a Significant Role in Enzymatic Catalysis? A Theoretical Analysis of Formate Dehydrogenase

Maite Roca,[b] Mónica Oliva,[a] Raquel Castillo,[a] Vicente Moliner,*[a, c] and Iñaki Tuñón*[b]

Abstract: A theoretical study of the protein dynamic effects on the hydride transfer between the formate anion and nicotinamide adenine dinucleotide (NAD^+), catalyzed by formate dehydrogenase (FDH), is presented in this paper. The analysis of free downhill molecular dynamic trajectories, performed in the enzyme and compared with the reaction in aqueous solution, has allowed the study of the dynamic coupling between the reacting fragments and the protein or the solvent water molecules, as well as an estimation of the dynamic effect contribution to the catalytic effect from calculation of the transmission coefficient in the enzyme and in solution. The obtained transmission coefficients for the enzyme and in solution were 0.46 ± 0.04 and 0.20 ± 0.03, respectively. These values represent a contribution to catalysis of 0.5 kcal mol^{-1}, which, although small, is not negligible keeping in mind the low efficiency of FDH. The analysis of the reactive trajectories also reveals how the relative movements of some amino acids, mainly His332 and Arg284, precede and promote the chemical reaction. In spite of these movements, the time-dependent evolution of the electric field created by the enzyme on the key atoms of the reaction reveals a permanent field, which reduces the work required to reach the transition state, with a concomitant polarization of the cofactor. Finally, application of Grote–Hynes theory has allowed the identification of the modes responsible for the substrate–environment coupling, showing how some protein motions take place simultaneously with the reaction. Thus, the equilibrium approach would provide, in this case, an overestimation of the catalyzed rate constant.

Keywords: dynamic effects · enzyme catalysis · FDH · Grote–Hynes theory · molecular dynamics · rare-event trajectories

Introduction

Enzymes are biological catalysts that allow organisms to carry out biological reactions on timescales compatible with life, speeding up chemical reactions by a factor of 10^6 to 10^{20}, which represents an amazing enhancement of chemical kinetics with respect to any synthetic catalyst. Moreover, these catalysts are not only very efficient, but they are usually specific. The origin of these features is a question of debate that has not yet had a conclusive answer. In order to obtain an answer to this difficult question, computer simulations have been demonstrated to be a powerful tool, complementary to experimental techniques such as NMR, single-molecule kinetics, kinetic isotope effects, site-directed mutagenesis, molecular engineering techniques, and so on. Many different computational approaches and models have been developed and applied with successful results, and it seems that a dynamic description of the enzyme-catalyzed process with flexible molecular models is required in order to obtain a realistic picture of the conformational changes of the protein and the chemical reaction at atomic level. Nevertheless, as pointed out by Benkovic et al.,[1] knowledge of the coupling between these two phenomena, as well as their chronological order, is still in an early stage of development, despite being indispensable for understanding these amazing catalysts. In this regard, Warshel et al.[2] stated that in the

[a] Dr. M. Oliva, Dr. R. Castillo, Prof. V. Moliner
Department de Química Física i Analítica
Universitat Jaume I, 12071 Castellón (Spain)
Fax: (+34) 964728066
E-mail: moliner@uji.es

[b] Dr. M. Roca, Prof. I. Tuñón
Department de Química Física, Universitat de València
46100 Burjassot, València (Spain)
Fax: (+34) 963864564
E-mail: Ignacio.tunon@uv.es

[c] Prof. V. Moliner
Institute of Applied Radiation Chemistry
Technical University ofŁódź, 90-924Łódź(Poland)

Supporting information for this article is available on the WWW under http://dx.doi.org/10.1002/chem.201000635.

examination of dynamical proposals there is a tendency to describe different views of the catalytic role of the enzyme dynamics as semantic issues. The origin of this lack of agreement probably lies in the fact that protein dynamics present an enormous complexity, and it can be difficult to define and quantify the effects on the reaction rate constant. In fact, the impact of protein dynamics on chemical reactivity can range over quite different phenomena. For instance, it is well known that many enzymatic processes are controlled by substrate binding or product release. Here, protein mobile loops can act as the gates to the active site, and then their motion can be the rate-determining step.[3] In other enzymes, the binding of the substrate can promote conformational changes in the enzyme that are needed to place some catalytic residues correctly.[4] Recent single-molecule experiments have shown that different conformational states of a particular enzyme can actually function as independent enzymes with noticeably different reaction rate constants.[5–8] In this case the dynamics associated with the interconversion between conformational states can determine the global rate constant.[9,10] However, probably the most intriguing question is whether the dynamics of the protein structural fluctuations are on the same timescale as the chemical step, thus being coupled to the reaction coordinate and influencing catalysis. In this regard, the role of protein motions in enzyme catalysis has been the topic of many experimental and theoretical studies in recent years,[11–19] with no consensus as to whether they can be considered as crucial for the catalysis.[2,20–23]

In this paper we focus on the influence of environment dynamic effects on the chemical step of an enzymatic reaction. Then, dynamic effects should be understood as the influence of environmental modes (i.e., all those modes that are different to the reaction coordinate) on the fate of reaction trajectories. The influence of these modes on the reaction clearly depends on the degree of coupling with the reaction coordinate, but it is also modulated by the characteristic frequencies of the modes. These dynamic effects of the environment on the reaction rate constant of the chemical step can be analyzed and quantified as the departures of the rate constant from the prediction based on transition state theory (TST),[24–26] that is, evaluating the transmission coefficient $\kappa(T)$ and whether this value is higher in enzymes than in solution. Then the rate constant can be presented by the well-known expression shown in Equation (1).

$$k(T) = \kappa(T) k_{TST}(T) \quad (1)$$

The origin of this coefficient being lower than unity is that the coupling of the reaction coordinate with the remaining coordinates is responsible for the existence of recrossings. These are trajectories that come back to the reactant state once they have crossed the transition state (TS), dividing the surface towards the products valley without equilibrating in that valley. As discussed below, the influence of each environmental mode on the transmission coefficient can be analyzed in terms of the coupling to the reaction coordinate and the value of its characteristic frequency.

In order to estimate the transmission coefficient, molecular dynamics (MD) trajectories starting from the TS with thermal distribution velocities can be monitored. Recent studies carried out in our group on different enzyme-catalyzed reactions (the methyl transfer from *S*-adenosylmethionine to catecholate in catechol *O*-methyltransferase, or to glycine in glycine *N*-methyltransferase, and the Michael addition catalyzed by chalcone isomerase),[21–23] compared with the respective reference reactions in solution, revealed that the values obtained in the enzyme are closer to unity (over 0.80) than the ones obtained in solution (over 0.60). Moreover, we have shown that Grote–Hynes (GH) theory,[21,23] based on the generalized Langevin equation,[27–29] can also give a very accurate estimation of the transmission coefficient of enzymatic reactions for nonquantum particles. The use of GH theory allows a deeper understanding and characterization of the coupling between the reaction and protein dynamics. The analysis of the friction kernel $[\zeta(t)]$, which gives the time correlation function of the fluctuating forces acting on the distinguished reaction coordinate, provides an efficient way, in the context of GH theory, to quantify the coupling of the remaining degrees of freedom of the system with the selected reaction coordinate.[27] This theory thus provides a direct connection between the effect of environmental modes and chemical kinetics through the transmission coefficient.

In this work, we have carried out a theoretical study of the protein motions in the rate-limiting step of the formate dehydrogenase (FDH EC 1.2.1.2), as well as an estimation of the dynamic contributions to lower the free-energy barrier. The enzyme FDH is widespread in nature, and it plays an important role as it is one of the best enzymes for cofactor regeneration in the processes of chiral synthesis with $NAD(P)^+$-dependent oxidoreductases.[30] Moreover, FDH has the biotechnological potential for use in organic acid synthesis as a catalyst in coenzyme regeneration systems for production of high-added-value pharmaceutical products.[31,32] Site-directed mutagenesis studies on FDH have been also carried out with the aim of transforming coenzyme specificity, as well as increasing its turnover frequency factor or its thermal stability.[33] To this end, a detailed knowledge of the catalytic mechanism of FDH at the molecular level could provide guidelines for future protein engineering on this enzyme.

FDH catalyzes the oxidation of the formate ion to carbon dioxide with the concomitant reduction of NAD^+ to NADH (Scheme 1), which means that charge separation is annihilated during the reaction progress. This hydride transfer seems to be the sole rate-limiting step in the catalytic mechanism of FDH.[34–36] The observed rate constant of $7.3\ s^{-1}$,[37,38] shows that it is an enzyme of relatively low efficiency compared with other NAD^+-dependent dehydrogenases, probably owing to strong interactions between the charged substrate in its ground state and several residues of the active site.[39] Thus, it has been shown that the most important residues for formate binding could be Arg284 and Asn146, or,

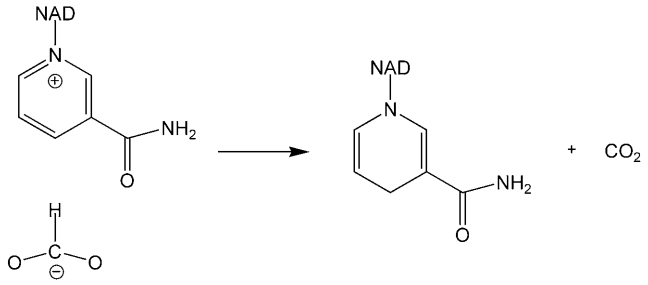

Scheme 1.

alternatively, His332 and Asn146. This very-well-organized active site of FDH has also been demonstrated by Kohen and co-workers[40] in their work on the temperature dependence of the intrinsic kinetic isotope effects (KIEs) and infrared photon-echo measurements of picosecond and femtosecond dynamics on the ternary complex of FDH with a cofactor, and the azide as the transition-state analogue.

Site-directed mutagenesis studies on FDH carried out by Popov and co-workers[41] showed that the His332/Gln313 pair is essential for enzyme activity, and confirmed the previous conclusions derived from X-ray diffraction structures[42] that Arg284 is directly involved in substrate binding, as well as supporting the catalytic conformation of the enzyme active site.[43] Recent structures of the apo and holo forms of *Moraxella sp.* strain C-1 (MorFDH), reported by Popov and co-workers, support the hypothesis that the catalytic residue His332 can form a hydrogen bond to both the substrate and the transition state.[44]

Regarding the interactions between the active site and the NAD^+, it has been suggested that nicotinamide ring of the cofactor can interact through hydrogen bonds with Thr282, Asp308, Ser334, and Gly335.[42] These residues would stabilize the initially positively charged ring, enhancing the electrophilic properties of the C4 atom by twisting the carboxamide group with respect to the pyridine plane, and thus perturbing the ground state.[42]

More recently, we published a theoretical study of the hydride-transfer step catalyzed by FDH, carried out by using hybrid quantum mechanics/molecular mechanics (QM/MM) techniques, but with the intrinsic assumption of equilibrium between the protein and the reaction coordinate.[45] The analysis of the free-energy profiles obtained in the enzyme, and comparison with that for the reaction in solution, suggested that the enzyme compresses the substrate and the cofactor into a conformation close to the transition structure by means of favorable interactions with the amino acid residues of the active site, thus facilitating the relative orientation of donor and acceptor atoms to favor the hydride transfer. By contrast, in water the TS is destabilized with respect to the reactant species because the polarity of the solute diminishes as the reaction proceeds, and consequently the reaction field, which is adapted to the change in the solute polarity, is also decreased. Therefore, protein structure is responsible for both effects, that is, substrate preorganization and TS stabilization with respect to the aqueous solution, thus diminishing the activation barrier.[45]

The present study aims to gain a deeper insight into the coupling between the enzyme motions and the chemical reaction. The question of whether the protein motions promote the chemical reaction, or if the enzyme remains frozen or in equilibrium with the substrate along the reaction, will be addressed. We will estimate the contribution of the dynamic effects on the rate constant enhancement from transmission coefficient calculation both in the enzyme and in aqueous solution. Application of Grote–Hynes theory to the calculation of the transmission coefficient will allow us to obtain the friction spectrum and identify the modes responsible for the substrate–environment coupling.

Computational Details

Hybrid QM/MM potentials of mean force: A QM/MM approach has been used in this study, with details of the computational model given elsewhere.[45] Briefly, the QM region consists of the formate anion together with the nicotinamide and ribose rings of the nicotinamide adenine dinucleotide (NAD^+) cofactor (33 atoms, as depicted in Figure 1), which is described by using the AM1 Hamiltonian.[46]

The initial coordinates of the protein were taken from the

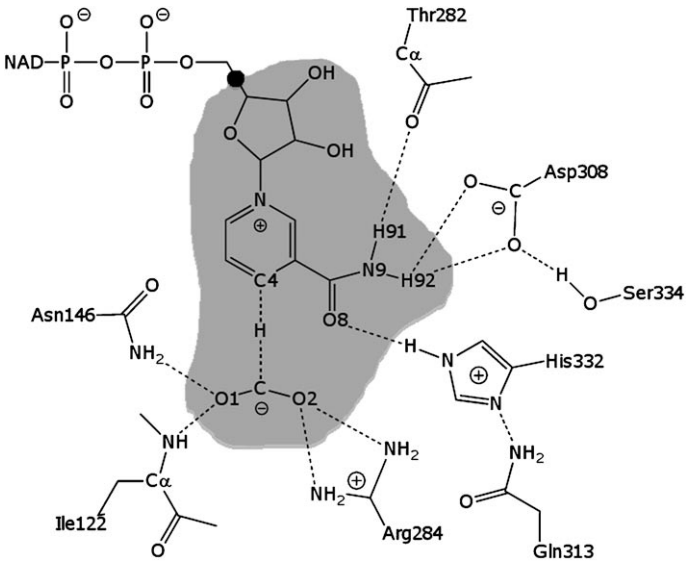

Figure 1. Detail of the FDH active site. Gray region corresponds to the QM subset of atoms, and the link atom is indicated as ●.

X-ray crystal structure of the *Pseudomonas sp.* complexed with the azide inhibitor in the formate binding site with PDB code 2NAD.[42] Once the azide molecule was replaced by the product of the FDH-catalyzed reaction, CO_2 and hydrogen atoms were added, and the system was placed inside a water molecule cubic box of side dimension 80 Å, centered on the C4 atom of the cofactor of subunit B. Because of the size of the system, all the residues further than 38 Å from C4 of the cofactor were removed, and those found fur-

ther than 18 Å from the same atom were kept frozen (20314 from a total of 23919 atoms). The MM subsystem was then described by using the OPLS-AA[47,48] and TIP3P[49] force field, as implemented in the fDYNAMO program.[50] To saturate the valence of the QM/MM frontier we used the link atoms procedure.[51,52] To treat the nonbonding interactions, a switch function with a cutoff distance in the range of 8–12 Å was used. The reaction was also studied in aqueous solution. In this case, the simulated system was formed by the formate anion together with the nicotinamide and ribose rings of the nicotinamide adenine dinucleotide (NAD^+) cofactor, the QM part, and a cubic box of water molecules (55.8 Å side). The QM region is the same as the one in the enzyme, and it was also described by using the AM1 semiempirical Hamiltonian. The MM region is composed of 5509 water molecules described by means of the TIP3P force field. To treat the nonbonding interactions, periodic boundary conditions were applied by using a switch function with a cutoff distance in the range of 8–12 Å.

The potentials of mean force (PMFs) were obtained in the NVT ensemble by using the antisymmetric combination of the distances describing the breaking and forming bonds, that is, d(C–Ht)–d(Ht–C4) (see Figure 1) as the distinguished reaction coordinate in both media.[45] A time step of 0.5 fs was used all around the simulations because the chemical step involves a hydrogen transfer. The Verlet algorithm was used to update the velocities,[53,54] and the reference temperature was 300 K. For all the calculations we employed the fDYNAMO program.[50]

As a first step in our analysis, we traced the AM1/MM PMFs in aqueous solution and in the enzyme for only a small range of reaction coordinate (RC) values (about ± 0.1 Å around the free-energy maxima found in our previous work)[45] by using the weighted histogram analysis method (WHAM) combined with the umbrella sampling approach.[55,56] These PMFs can be satisfactorily fitted to a parabolic expression, as given in Equation (2).

$$\Delta PMF = -\frac{1}{2}K_{eq}(RC - RC^{\ddagger})^2 \quad (2)$$

The purpose of these PMFs is to obtain a good estimation of the TS position in terms of the antisymmetric reaction coordinate, $RC^{\ddagger}$, and also to obtain the equilibrium barrier frequency ω_{eq} necessary for the Grote–Hynes (GH) analysis. This is the barrier frequency under the assumption of equilibrium between the reaction coordinate and the remaining degrees of freedom, and is given by Equation (3), in which μ_{RC} is the reaction coordinate reduced mass and c is the speed of light.

$$\omega_{eq} = \frac{1}{2\pi c}\sqrt{\frac{K_{eq}}{\mu_{RC}}} \quad (3)$$

In order to obtain these PMFs in the TS neighborhood (shown as Supporting Information) we ran 10 simulation windows, changing the reference value of the reaction coordinate in the umbrella potential by only 0.01 Å. The force constant applied to the reaction coordinate in these simulations was 2000 kJ mol^{-1} Å^{-2}. From the parabolic fit, we estimate that the equilibrium barrier frequencies (ω_{eq}) are 4120 cm^{-1} in aqueous solution and 2160 cm^{-1} in the enzyme. The maxima of the PMFs are located at -0.13 and -0.14 Å in aqueous solution and in the enzyme environment, respectively.

Free downhill trajectories: We ran a 750 ps NVT MD trajectory restrained in the TS region with a time step of 0.5 fs for the reaction system both in aqueous solution and in the enzyme. The simulation temperature was 300 K and one configuration was saved every 5 ps, resulting in 150 configurations that were used to compute free downhill trajectories. The velocity associated with the reaction coordinate is not properly thermalized in these configurations. Thus, following a procedure similar to that used by Gao and co-workers[57] and used in our previous studies,[21,23] we selectively removed the projection of the velocity on the reaction coordinate, and added a random value taken from a Maxwell–Boltzmann distribution just for the atoms involved in the reaction coordinate.

For each of the saved configurations with modified velocities we ran free NVE simulations integrating the equations of motion forward and backward, just changing the sign of the velocity components.[58] Downhill trajectories were propagated from -8 to $+8$ ps in the enzyme, and from -2 to $+2$ ps in aqueous solution, by using a time step of 0.5 fs in both environments. The trajectories obtained in the enzyme and in solution were then classified as reactive trajectories when the reactants connect to products (RP trajectories), and nonreactive trajectories that lead either from reactants to reactants (RR) or from products to products (PP). Both reactive and nonreactive trajectories may exhibit recrossings of the dividing surface. To compute the transmission coefficient we used the "positive flux" formulation,[59] by assuming that the trajectory was initiated at the barrier top with forward momentum along the reaction coordinate. For a given time t, with $t=0$ being the starting time for the downhill trajectory, the time-dependent transmission coefficient can be calculated as shown in Equation (4), in which j_+ is the initial positive flux at $t=0$, and $\theta(RC)$ is a step function equal to 1 on the product side of the reaction coordinate and 0 on the reactant side. The average was calculated over all the trajectories.

$$\kappa(t) = \frac{\langle j_+\theta[RC(+t)]\rangle - \langle j_+\theta[RC(-t)]\rangle}{\langle j_+\rangle} \quad (4)$$

Application of GH theory: GH theory can be applied to describe the evolution of the system along the reaction coordinate in the TS. In particular, the transmission coefficient can be obtained as the ratio between the reactive frequency and the equilibrium barrier frequency,[60] as shown in Equation (5), in which the reactive frequency ω_r is obtained from the GH equation [Eq. (6)].[28,29]

$$\kappa_{GH} = \frac{\omega_r}{\omega_{eq}} \tag{5}$$

$$\omega_r^2 - \omega_{eq}^2 + \omega_r \int_0^\infty \zeta_{TS}(t) e^{-\omega_r t} dt = 0 \tag{6}$$

In GH theory the friction kernel is obtained at the TS ($\zeta_{TS}(t)$) to determine the forces exerted during the passage over the top of the barrier, by assuming that recrossings take place in the proximity of this dynamic bottleneck.[27,29] This expression is given in Equation (7), in which $F_{RC}(t)$ is the force on the reaction coordinate, and μ_{RC} is the associated reduced mass.

$$\zeta(t) = \frac{\langle F_{RC}(0) F_{RC}(t) \rangle}{\mu_{RC} k_B T} \tag{7}$$

The analysis of the friction kernel ($\zeta(t)$), which gives the fluctuating forces acting on the reaction coordinate, provides an efficient way to quantify the coupling of the remaining degrees of freedom of the system with the selected reaction coordinate.[27]

For the evaluation of the TS friction kernel, we ran 50 ps of constrained MD simulations at the top of the PMF, by using a Wilson's matrix-based RATTLE-like velocity–Verlet algorithm.[53,61] A very small time step of 0.01 fs was used to ensure the convergence of the algorithm, and the forces acting on the reaction coordinate were saved at each simulation step.

GH theory includes the frozen-environment approach as a limiting case (also called the nonadiabatic limit).[60] If the rest of the coordinates can be considered to be frozen compared with the motion of the reaction coordinate in the passage through the TS,[62,63] then the friction kernel can simply be replaced by its zero-time value, and the reaction frequency under the frozen-environment approach (ω_{fe}) is then given by Equation (8).

$$\omega_{fe}^2 - \omega_{eq}^2 + \zeta_{TS}(t=0) = 0 \tag{8}$$

Another interesting limit is the Kramers regime,[64] under which it is assumed that all the friction is exerted during the barrier crossing, that is, the timescale of the friction kernel is shorter than the inverse of ω_r.[60] In this situation, the GH equation can be rewritten as Equation (9).

$$\omega_{Kr}^2 - \omega_{eq}^2 + \omega_{Kr} \int_0^\infty \zeta_{TS}(t) dt = 0 \tag{9}$$

Results and Discussion

Time-dependent transmission coefficients: After randomizing the reaction coordinate velocity for each of the 150 saved configurations, as described in the previous section, we ran free hybrid QM/MM MD simulations, allowing the system to evolve downhill trajectories from the TS. Analysis of the trajectories indicated that, in the enzyme, 61 were reactive trajectories of the RP type, and the rest were nonreactive: 30 of RR type and 59 of PP type. In solution, 23 trajectories were of the RP type, 59 of RR type, and 68 of PP type. As observed, it seems that the protein environment assists the chemical system in crossing the barrier successfully from the reactants to the products valley more efficiently than the water molecules of the aqueous solution.

The time-dependent transmission coefficients, evaluated by using the "positive flux" formulation [Eq. (4)], are presented in Figure 2. The evolution of $\kappa(t)$ shows a fast decay

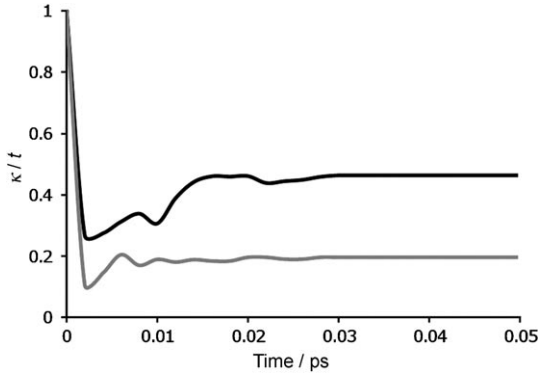

Figure 2. Time-dependent transmission coefficients obtained in the enzyme (black line) and in aqueous solution (gray line).

in both media during the first 3 fs, reaching a plateau after 10 fs in aqueous solution, and after 20 fs in the enzyme environment. The solution and enzyme values of the transmission coefficient measured in this time-independent region are $\kappa_{aq} = 0.20 \pm 0.03$ and $\kappa_{enz} = 0.46 \pm 0.04$, respectively. The first conclusions that can be derived from these values are that the transmission coefficient is larger in the enzyme than in solution, and its contribution to the catalytic effect, though small, is not negligible ($\kappa_{enz}/\kappa_{aq} = 2.3$). According to our previous study,[45] free-energy lowering computed on the assumption of equilibrium between the reaction coordinate and the environment provided a value of 8.9 kcal mol^{-1} (the AM1/MM free-energy barriers obtained from the aqueous solution and enzymatic PMFs were 21.3 and 12.4 kcal mol^{-1}, respectively). The contribution of dynamic effects to the total catalytic effect, which can be estimated from the expression given in Equation (10), makes a contribution of about 0.5 kcal mol^{-1} at 300 K.

$$\Delta\Delta G_{dyn} = -RT \ln\left(\frac{\kappa_{enz}}{\kappa_{aq}}\right) \tag{10}$$

This value represents around 5% of the total catalytic effect evaluated as the addition of the equilibrium and transmission coefficient contributions to the rate constant at 300 K. Moreover, the values of the transmission coefficients, and in particular the one obtained in the enzyme, are significantly smaller than those obtained in previous studies on

different enzymes.[21–23] This probably means that, although the selected reaction coordinate captures the essence of the reaction, important changes take place in the protein coupled with the hydride transfer.

Analysis of rare-event trajectories: Figure 3 shows the time evolution of the key interatomic distances involved in the hydride transfer. The time $t=0$ corresponds to the passage

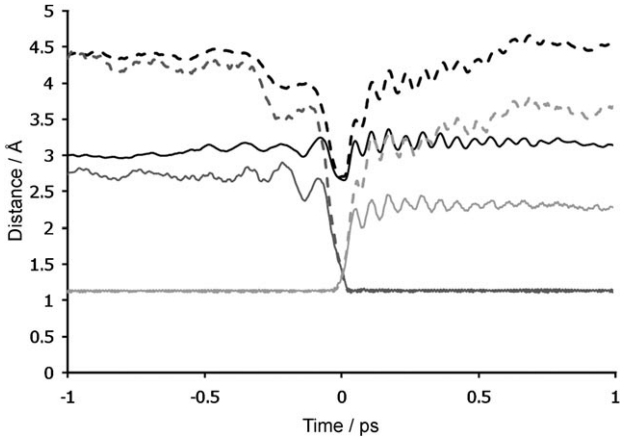

Figure 3. Time evolution of key interatomic distances obtained in the enzyme (solid lines) and in solution (dashed lines); C4···C (black line), C4···Ht (dark-gray line) and C···Ht (light-gray line). Only the −1 to +1 ps evolution is shown. The behavior at earlier and later times does not show any significant variation.

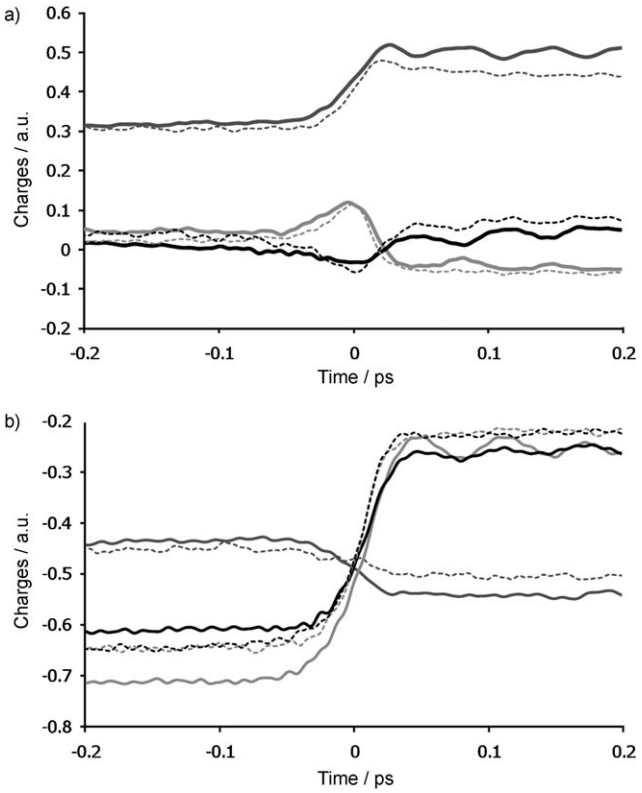

Figure 4. Mulliken charges averaged over reactive trajectories for a) C4 (light-gray line), C (dark-gray line), Ht (black line); and b) O8 (dark-gray line), O1 (light-gray line) and O2 (black line). Solid lines correspond to the enzymatic reaction and dashed lines to the aqueous solution reaction.

of the system over the barrier top, negative times correspond to the evolution of the system towards the reactant valley, and positive times towards the product valley. Values were averaged over the set of successful RP trajectories.

It can be observed that the reaction proceeds by an approaching of the donor and acceptor carbon atoms, with a concomitant transfer of the hydride atom. In fact, the distance between the two carbon atoms reaches a minimum in the TS. All of these geometrical changes take place in a synchronous way from −0.3 to +0.5 ps in solution, whereas in the enzyme the process takes place in a shorter time, starting at −0.1 ps and arriving at a stationary situation at +0.2 ps. Figure 3 also shows that, although distances corresponding to nonbonded distances are longer in solution than in the enzyme (see C4···C and C4···Ht in the reactants and C4···C and Ht···C in the products), those values corresponding to standard bond lengths are equal in both media and, even more interesting, the values appearing at the TSs are not dependent on the environment.

Figure 4 presents the evolution of the reaction from the electronic point of view, displaying the averaged Mulliken charges on selected atoms for the process in aqueous solution and in the enzyme. Although these charges must not be considered absolute values, their time evolution is a good guide to the electronic redistribution taking place in the substrate and the cofactor. As explained previously, the reaction proceeds with charge separation annihilation: the formate and the cofactor (the nicotinamide ring) have formal charges of −1 and +1 a.u., respectively, in the reactant state and of zero in the product state. The results presented in Figure 4 clearly demonstrate how the charge-distribution changes take place in a very short time, between −0.05 and +0.03 ps around the TS. The oxygen atoms of the formate lose negative charge during the reaction as well as the carbon atom, reflecting the aforementioned change in the formal charge of the substrate. It is important to underline the negative charge of the transferred hydrogen atom in the TS, concurrently with the maximum positive charge reached by the acceptor atom, C4. As shown by the evolution of the charge on the O8 atom in Figure 4, the cofactor is polarized, producing an increase of the negative charge on this atom and a positive charge on the C4 atom, which reaches its maximum just on the TS. These changes on the cofactor start before the variations reported for the charges of the formate atoms. As discussed below, movements of some residues of the active site must promote these changes. It is important to point out that the charge evolution on C4 and O8 obtained in solution are not as favorable for the hydride transfer as in the enzyme; the increase in the positive charge of the former starts at a slightly more advanced stage of the reaction, whereas the O8 atom in solution is clearly less polarized than in the enzyme.

Whereas until now our analysis has been focused solely on the geometrical and electronic processes taking place on the substrate and the cofactor, these have to occur coupled to changes in the environment, either on the solvent molecules or the protein residues. Figure 5 shows the time evolution of intermolecular distances between key atoms of the substrate or cofactor and of the amino acids of the enzyme, averaged over the reactive trajectories. It can be observed how the distance between Asp308 and the amino group of the cofactor is increased as soon as the TS is reached. This change may be a response to the annihilation of the positive charge on the cofactor due to the hydride transfer. Other distances that elongate from reactants to products are those established between one of the oxygen atoms of the formate and Arg284. Interestingly, these two distances, and in particular the one that defines the strongest hydrogen bond interaction, O1···HH12Arg284, increases significantly before arriving at the TS, thus anticipating the electronic and geometrical changes occurring in the substrate and the cofactor. A similar behavior, and perhaps even more dramatic, is observed for the time evolution of the distance between the carbonyl oxygen of the nicotinamide ring of the cofactor, O8, and His332. The relative motions of this residue appear to be already activated about 0.5 ps before reaching the TS. The approach of this residue to the cofactor polarizes the carbonyl group of the cofactor, which provokes an increase of the positive charge on C4, as reflected by the evolution

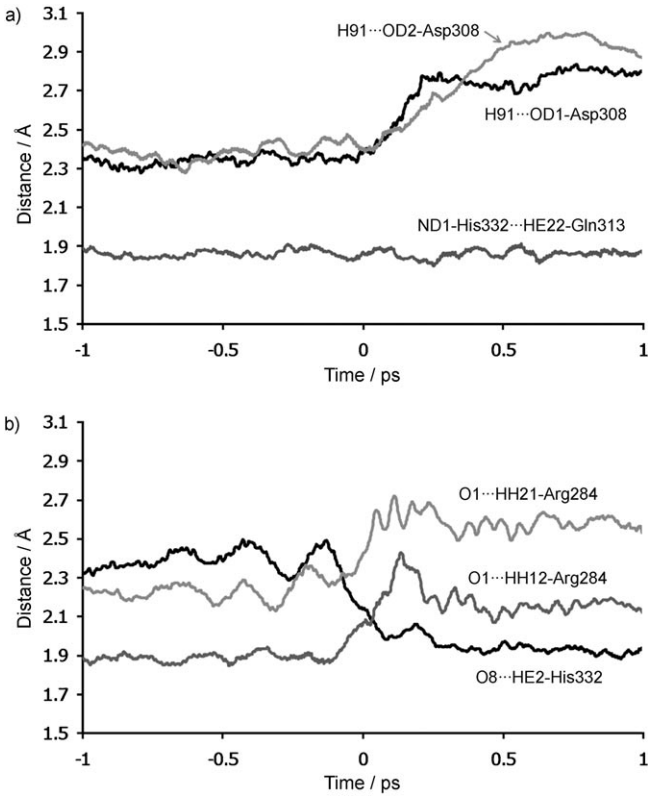

Figure 5. Time evolution of intermolecular distances between the substrate or cofactor and the amino acids of the enzyme averaged over reactive trajectories.

of the partial charge on O8 and C4 shown in Figure 4. This electronic effect takes place within a twisting of the full carboxamide group with respect to the pyridine ring, thus perturbing the ground state as proposed by Lamzin et al.[42]

The behavior of the binary His332···Gln313 is also particularly interesting: the almost invariant distance established between these residues suggest a global movement on the protein, which facilitates the interaction of the His332 with the carbonyl group of the formamide moiety of the nicotinamide ring. The importance of this His332···Gln313 interaction is in agreement with the site-directed mutagenesis performed by Popov and co-workers, which showed how His332Phe mutation leads to a complete loss of enzyme activity.[41]

A similar study can be carried out for the reaction in solution by exploring the time evolution of the distance between selected atoms of the reacting system and an atom of the closest water molecule. This analysis reveals that intermolecular interactions established between the reacting system and the environment change as the hydride transfer proceeds, but these changes seem to be a consequence of the charge reorganization.

Another comparison between the aqueous solution and the enzyme can be made by using a global coordinate, such as the electric field created by the environment. With this purpose we analyzed the time-dependent evolution of the electric field created by the protein or the aqueous solution on the substrate and cofactor along the reactive trajectories. The modulus of the electric field created by both media on Ht, C, and C4 averaged over the reactive trajectories is depicted in Figure 6. As observed in the figure, the electric fields created by the two media present different behaviors. The first conclusion that can be derived from Figure 6 is that the electric field created by the protein is more robust than that created by the water molecules. Thus, in solution, the modulus is almost invariant until it reaches the TS, upon which it decreases noticeably in a few femtoseconds to reach a permanent value once more. This behavior can be readily understood in terms of a reaction field that is adapted to the changes in the electronic distribution of the solute as the reaction proceeds, thus decaying as the polarity of the QM system diminishes from reactants (two separated charged species) to products (neutral species). Also, the fact that the stationary situation was reached once the TS had been achieved reveals a very flexible environment in which the molecules are reoriented very easily. In contrast, the electric field created by the enzyme remains essentially invariant when the system evolves from reactants to products. This feature was, a priori, not expected, keeping in mind the significant movements of the amino acids previously observed in the reactive trajectories. Nevertheless, it seems that those movements take place in such a way that the electric field is not altered, and it is oriented in such a way that the hydride transfer is favored. This feature can be better understood by combining the information on the evolution of the electric field (Figure 6) with the evolution of charge distribution (Figure 4). Thus, although the reaction is not fa-

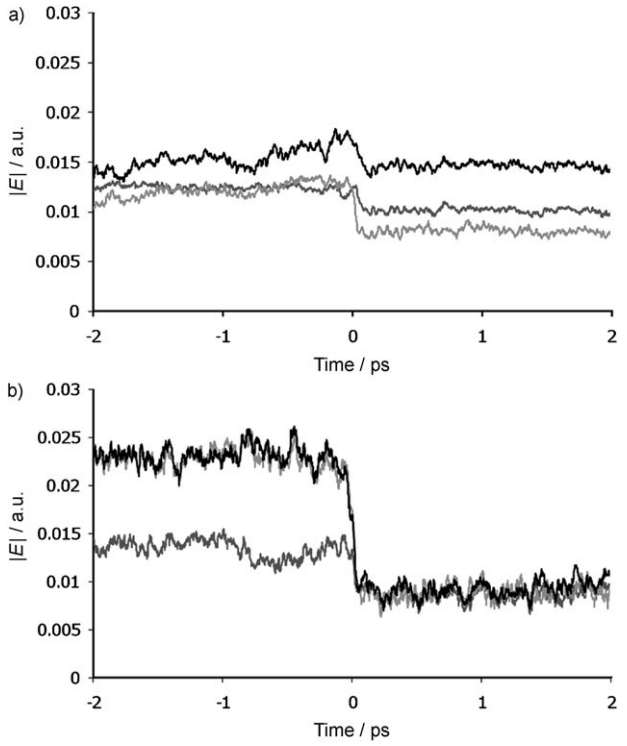

Figure 6. Time-dependent evolution of the modulus of the electric field on the Ht (black line), C (light-gray line) and C4 (dark-gray line) created by the enzyme (a) and by the aqueous solution (b).

vorable in either of the two media from an electrostatic point of view (due to the fact that it represents the annihilation of two charged species perfectly solvated in both media), the resulting pattern of electric forces created by the environments are significantly less unfavorable in the protein than in aqueous solution. In free-energy terms, this means that a larger free-energy penalty needs to be paid for the reaction in solution than in the cavity of the enzyme, because the charged species are neutralized in a polar medium. In the enzyme, this penalty does not appear, given that the electric field seems to be already suited to accommodate the charge distribution of the TS more than that of the reactant state; as shown in Figure 6, a maximum of the electric field on the Ht position is observed on the TS.

Results of GH theory: Although the analysis of reactive trajectories can inform us about some of the details of the chemical reaction, it is clearly limited by the number of variables that can be analyzed. A complementary approach is the use of the friction kernel [see Eq. (7)] in the context of GH theory as a source of information about the coupling of the reaction coordinate to all the remaining degrees of freedom. Of course, such a use should first be validated by comparison of the transmission coefficients obtained from the GH theory with those already determined from MD (see above).

Once the equilibrium frequency ω_{eq} is known from Equation (3), we need to evaluate the friction kernel to calculate the transmission coefficient. The normalized autocorrelation functions (ACFs) of the forces acting on the reaction coordinate at the TS ($\langle F_{RC}(0)F_{RC}(t)\rangle_{TS}$) obtained in water and in the enzyme show a remarkably similar global time evolution in both media (see the Supporting Information). Nevertheless, although the time evolution is quite similar in both environments, the zero-time values of the un-normalized ACF [Eq. (7)] are different. The initial friction can be expressed as a wavenumber according to Equation (11).

$$\omega_{\xi} = \frac{1}{2\pi c}[\zeta_{TS}(t=0)]^{1/2} \tag{11}$$

This initial friction frequency is 4867 cm^{-1} in aqueous solution and 2691 cm^{-1} in the enzyme. As in other enzymatic reactions previously analyzed, the coupling between the reaction coordinate and the remainder of the system is stronger in solution than in the enzyme.[21–23] The larger value of the friction in solution with respect to the enzymatic value reflects that a larger reorganization of the environment occurs, coupled to the changes in the charge distribution of the substrate along the reaction.[21–23]

Due to the fact that the subsequent analysis will be performed within the framework of GH theory, it is important to check if GH theory is able to reproduce quantitatively the transmission coefficients obtained from MD simulations. The obtained values for the reaction frequencies [Eq. (6)] in aqueous solution and in the enzyme were $\omega_{r,aq} = 1090\ cm^{-1}$ and $\omega_{r,enz} = 812\ cm^{-1}$, respectively. By using these frequencies and Equation (5) the calculated GH transmission coefficients are $\kappa_{GHaq} = 0.27 \pm 0.06$ and $\kappa_{GH,enz} = 0.38 \pm 0.02$. The results are in excellent agreement with the MD values. This encouraging result clearly shows that GH theory is applicable to enzymatic reactions even in the case of the transfer of classical light particles. Interestingly, when the frozen environment is applied [Eq. (8)], the GH theory provides an imaginary number for the transmission coefficients, both in water and in the enzyme: $\kappa_{GH,aq} = 0.63i$ and $\kappa_{GH,enz} = 0.74i$. This is due to an overestimation of the friction, resulting in a trapped TS configuration. It is also worth mentioning that Kramers regime,[64] [Eq. (9)], which considers an instantaneous frictional response of the system to the movement along the reaction coordinate, gives a seriously underestimated result for the transmission coefficient: 0.10 and 0.002 for the reaction in the enzyme and in solution, respectively.

Once the validity of GH theory to describe the classical hydride transfer in FDH and in aqueous solution has been established, it is important to make a comment about the validity of the different approaches for modeling dynamic effects in chemical reactions, and the implications in the understanding of chemical reactions in complex environments. First, a transmission coefficient equal to unity corresponds to the equilibrium assumption, that is, that all the motions of the system have enough time to relax fully after any change in the selected reaction coordinate. This value is not completely unreasonable, but for this reaction provides an overestimation of the enzymatic rate constant, considering

that the values of the transmission coefficient obtained by MD or GH theory are smaller than unity. Instead, the Kramer regime, in which it is assumed that all the friction of the system on the reaction coordinate is exerted during the top of the barrier crossing, underestimates the rate constant. In this case the ratio between the Kramers and GH values are $\kappa_{Kr,enz}/\kappa_{GH,enz}=0.26$. More importantly, this frozen-environment approach, in which it is assumed that all the coordinates of the system but the reaction coordinate itself remain frozen during the passage over the barrier top, provides a completely wrong picture of the chemical process, both in the enzyme and in solution. This is particularly important given that this limit has been shown to work properly in other enzymatic and aqueous solution reactions.[60,65] Note that nowadays many theoretical studies of enzymatic reactions employ models with much reduced flexibility. According to our results this could lead to artifacts in the description of the chemical process. It should be stressed that, a priori, a chemical step that involves the transfer of a light atom, such as the hydride transfer studied here, could be considered a good example for the validity of the frozen-environment approach. Our results clearly demonstrate that some motions of the environment must be considered to take place simultaneously with the hydride transfer. Although the equilibrium approach can lead to a qualitative estimation of the changes occurring in the environment during the process, as made in our previous study on the FDH reaction,[45] dynamic effects must be incorporated to obtain a more realistic and quantitative description of the catalytic process.

The significant improvement obtained when using GH theory, as compared to its nonadiabatic limit or the frozen-environment approach, is clearly due to the ability of the former to incorporate the dynamics of the environment through a time-dependent friction kernel in a generalized Langevin equation. To understand the coupling between the reaction coordinate and the remaining degrees of freedom in more detail, we have analyzed this friction kernel, attempting to identify which motions participate most importantly in the reaction. For this purpose, we have calculated the friction spectrum as the Fourier transform of the friction kernel,[66] for the solution and enzyme reactions, by using Equation (12).

$$\zeta_{TS}(\omega)=\int_{-\infty}^{+\infty}\zeta_{TS}(t)e^{i\omega t}dt \qquad (12)$$

The environmental motions can then be classified according to their influence on the reaction coordinate, reflected in the intensity of the signal, and the value of their frequency as compared to the reaction frequency. Those motions, which present a frequency much larger than the reaction frequency are expected to contribute residually to the deviation of the transmission coefficient from unity because these motions have enough time to be fully relaxed during a change in the reaction coordinate. Otherwise, those motions with characteristic frequencies significantly smaller than the reaction frequency are expected to be unable to follow the changes in the reaction coordinate when the systems cross the dividing surface, and then they can successfully be described as frozen motions. Finally, those motions presenting frequencies of the same order as the reaction frequency are expected to be dynamically coupled to the reaction progress, and if they do present an important intensity then they should more properly be considered as part of a more complete reaction coordinate. Then, it can be more revealing to decompose the total friction spectrum into two different contributions: the relaxed spectrum ($\zeta^{+}(\omega)$) and the rigid spectrum ($\zeta^{-}(\omega)$), as given in Equations (13) and (14), respectively.[66]

$$\zeta^{+}(\omega)=\frac{\zeta_{TS}(\omega)}{\omega_{eq}}\left(\frac{\omega^2}{\omega_r^2+\omega^2}\right) \qquad (13)$$

$$\zeta^{-}(\omega)=\frac{\zeta_{TS}(\omega)}{\omega_{eq}}-\zeta^{+}(\omega) \qquad (14)$$

The important point is that the rigid spectrum accounts for the contributions of those motions that, while coupled to the reaction coordinate, can be considered as frozen during the passage over the barrier top. Then, this part of the friction is responsible for the deviations from TST (i.e., from a transmission coefficient equal to unity) in the nonadiabatic, frozen-environment limit. This deviation is due to the fact that these motions remain essentially inactive during the timescale of the reaction.[60] On the other hand, the relaxed spectrum reflects those motions coupled to the reaction coordinate that can dynamically respond to the changes in the TS region on the timescale of the reaction coordinate. These motions appearing in this spectrum are thus responsible for the deviations from the frozen-environment limit of the transmission coefficient.[66]

The rigid and relaxed spectra, calculated from the friction kernels obtained in water and in the enzyme, are shown in Figure 7. The rigid spectrum in water shows more intense lines than the corresponding spectrum in the enzyme, especially below 600 cm^{-1}. This low-frequency motion region of the spectrum corresponds in water to hindered translations, diffusion, reorientations of water molecules, and multimolecular motions, whereas in the enzyme this region contains highly collective motions.[67–69] The greater intensity of the water spectrum in this region indicates that the motions that should be considered essentially frozen are more strongly coupled to the reaction coordinate in solution than in the enzyme. As noted above, this can be related to the fact that many solvent molecules must be reordered as charged reactants are transformed into neutral products. The key feature of the present reaction is that the relaxed friction spectra, responsible for the departures from this frozen-environment approach, show strongly coupled motions in water, and even more in the enzyme. Effectively, it was already known that some motions (e.g., librations of water molecules) can at least partly follow the barrier crossing changes in the reaction coordinate.[66] These motions are largely responsible for

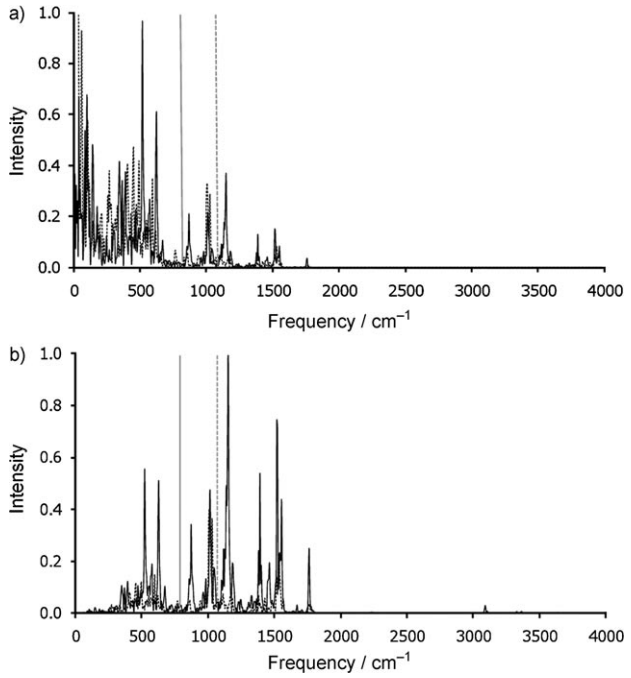

Figure 7. Rigid (a) and relaxed (b) friction spectra (intensity in arbitrary units) for the reaction in the enzyme (solid lines) and in aqueous solution (dashed lines). The reactive frequencies for both media are shown as vertical gray lines; solid and dashed for enzyme and solution, respectively.

the failure of the frozen-environment estimation of the transmission coefficient.

In order to assign the important signals in the friction spectra, we carried out a normal-mode analysis for a TS structure in solution and in the enzyme. The transition structures were obtained by using a micro/macro iteration approach in which the coordinate space is divided into a control space and a complementary space.[70–72] The Hessian matrix is defined only for the control space, whereas the complementary space is completely optimized by using gradients. In the definition of the control space, we included all those residues and water molecules directly interacting with the substrate. In aqueous solution, this definition of the control space included all the coordinates of the QM subsystem (33 atoms) and 42 TIP3P water molecules (all those water molecules found less than 8 Å from the C4 atom of the cofactor), resulting in a total of 228 atoms. In the enzyme, this definition included, in addition to the substrate molecule and the cofactor, the following residues: Asn146, Ile122, Arg284, His332, Gln313, Asp308, Thr282, and Ser334 (a total of 160 atoms). By combining the results of the normal-mode analysis with the friction spectra signals we have been able to identify several signals corresponding to internal rotations and relative movements of the surrounding water molecules or residues.

In aqueous solution the most intense signals appear at frequencies substantially smaller than the reaction frequency. The signals appearing from 50–100 cm^{-1} can be assigned to hindered translations, reorientations, and multimolecular motions of water molecules. The group of signals appearing between 250 and 600 cm^{-1}, which contribute essentially to the rigid spectrum, but also, to a minor extent, to the relaxed spectrum in water, can be associated with hydrogen bonds established between water molecules and the NH_2 moiety and O8 atom of NAD^+, and also with the O1 and O2 atoms of formate. Some signals appearing between 1010 and 1030 cm^{-1}, which contribute more or less equally to the rigid and the relaxed spectra, have been assigned to the out-of-plane motion of the ring hydrogen atoms of NAD^+, and especially to the sp^2 to sp^3 hybridization change of the C4 carbon atom. Two other minor signals appear in the relaxed spectrum at 1530 and 1750 cm^{-1}. The first one has been assigned to the stretching of the amide bond coupled also to the N–H bending, and the second one is due to the C7=O8 stretching. A very minor signal appearing about 3090 cm^{-1} has been assigned to C–H stretchings.

For the enzymatic reaction we can observe that more signals contribute in a significant way to the relaxed spectrum. This can be attributed in part to the fact that the reaction frequency in the enzyme is smaller than in solution. Interestingly the two most intense signals of the rigid spectrum, appearing at 520 and 630 cm^{-1}, also contribute significantly to the relaxed spectra. The first one can be assigned to the hydrogen bond established between His332 and O8, and the second one seems to be more properly assigned to a coupled motion of several hydrogen bonds involving Arg284 with O1 of formate, Asp308 and Thr282 with the NH_2 group of NAD^+, and also His332 with O8. These motions are somewhat slower than the reaction frequency itself and then they must precede the change in the distinguished reaction coordinate. However, they cannot be considered at all as frozen while the system crosses the dividing surface. This behavior is clearly reflected in the analysis of the reactive trajectories presented in Figure 5.

The signals appearing above the reaction frequency contribute more to the relaxed spectrum. The signals at 870 and 1010 cm^{-1} also involve hydrogen-bond interactions established between the substrate and the active site. The first one corresponds to the simultaneous change in the hydrogen bonds established between His332 and Gln313, and between His332 and O8 atom of the cofactor. The second one involves the hydrogen bonds established by Arg284 with the substrate and with the carbonyl oxygen atom of Ile122. The intense band located at 1140 cm^{-1} has been assigned to the out-of-plane bending of the hydrogen atoms of the pyridine ring NAD^+, and the sp^2 to sp^3 change of the C4 carbon atom. Other higher frequency bands have been assigned to intramolecular motions of the cofactor: the stretching of the amide bond coupled also to the N–H bending (1520 cm^{-1}), the C7=O8 stretching (1750 cm^{-1}), and to C–H stretching (3090 cm^{-1}).

In general, all these motions contribute to the passage of the system through the TS in the enzyme. Because the characteristic frequency of some environment vibrational modes is much lower than the reaction frequency, we can consider them essentially as frozen during the barrier crossing, but, as illustrated in Figure 5, they must be activated prior to the

passage of the system through the TS. Thus, this is a clear example of the fact that the participation of the environment motions in the reaction coordinate can be different at different stages of the reaction progress. A hypothetical success of the frozen-environment approach in reproducing the transmission coefficient, which is clearly not the case for FDH, as discussed above, would never imply that the environment could be viewed as static during the whole reaction process.

Conclusion

A QM/MM MD study of the protein dynamic effects on the hydride transfer between formate anion and nicotinamide adenine dinucleotide (NAD^+), catalyzed by the enzyme formate dehydrogenase (FDH), has been presented in this paper. From TS configurations obtained from the top of the free-energy barrier, free downhill molecular dynamics trajectories have been performed in order to carry out a comparative analysis of the dynamic behavior of both condensed media. The analysis of reactive and nonreactive trajectories in both environments has allowed the study of the dynamic coupling between the substrate and the cofactor with the protein or the solvent water molecules, as well as the estimation of the dynamic effect contribution to enhance the rate constant from calculation of the transmission coefficients in both media.

The analysis of the downhill trajectories on the protein reveals how the relative movements of some amino acids precede and promote the chemical reaction. In particular, the movements of His332, coupled with Gln313, facilitate the reaching of the TS by polarizing the carbonyl group of the nicotinamide ring of NAD^+, which provokes the increase of the positive charge of the acceptor carbon atom; meanwhile the distance between the substrate and Arg284 is also increased before arriving at the TS, thus displacing the negative charge of the carboxylate oxygen atoms of the formate towards the cofactor, helping the hydride to be transferred. The transmission coefficients obtained from MD simulations are 0.46 ± 0.04 and 0.20 ± 0.03 in the enzyme and in solution, respectively. These values represent a contribution to catalysis of 0.5 kcal mol^{-1}, which, though small, is not negligible keeping in mind the low efficiency of FDH. Moreover, these values, and in particular the one obtained in the enzyme, are significantly smaller than those obtained in previous studies on different enzyme-catalyzed reactions,[21–23] revealing important changes taking place in the protein coupled with the hydride transfer. Thus, the equilibrium approach, which in this case provides an overestimation of the enzymatic rate constant, can lead to qualitative estimations of the changes occurring in the environment during the process, but dynamic effects must be incorporated to obtain a quantitative description.

The time evolution of the electric field created by the two environments on the key atoms of the reaction reveals that in the enzyme it remains essentially invariant when the system evolves from reactants to products. This means that, although significant movements of the amino acids take place along the reactive trajectories, the electric field is not altered, and it is oriented in such a way that the hydride transfer is favored with respect to the reaction in solution. The aqueous solution, on the contrary, behaves as a force adapted to the electron distribution changes taking place along the chemical reaction. In free-energy terms, this means that a larger free-energy penalty needs to be paid for the reaction in a polar medium, such as the aqueous solution, than in the cavity of the enzyme. In the enzyme, this penalty does not appear, given that the electric field seems to be already suited to accommodate the charge distribution of the TS more than that of the reactant state.

Grote–Hynes theory has been applied to analyze the friction kernel, which has allowed the identification of some key vibrational modes that govern the coupling between the two different environments and the reaction coordinate, and, in particular, their relevance for the reaction to proceed in the protein medium, as deduced from the downhill trajectories. The results of the transmission coefficients obtained by means of the GH theory (0.38 ± 0.02 and 0.27 ± 0.06 in the enzyme and in solution, respectively) were in excellent agreement with the MD values, which show that this theory can be applied even for the case of the transfer of classical light particles as in the FDH case. Application of the different limits reveals that the frozen-environment approach, in which it is assumed that all the coordinates of the system but the reaction coordinate itself remain frozen during the passage over the barrier top, provides a completely wrong picture of the chemical process, both in enzyme and in solution. It should be stressed that, a priori, a chemical step involving the transfer of a light atom, such as the hydride transfer studied here, could be thought of as a good example of the validity of the frozen-environment approach. Our results clearly demonstrate that some motions of the environment must be considered to take place simultaneously with the hydride transfer.

The assignment of the important signals in the friction spectra has shown that the two most intense signals correspond to the hydrogen bond established between His332 and O8, and the second one to a coupled motion of several hydrogen bonds involving Arg284 with O2 of formate, Asp308 and Thr282 with the NH_2 group of NAD^+, and also His332 with O8. Because these motions are somewhat slower than the reaction frequency itself, they must be activated in advance of the passage of the system through the TS, as confirmed from the analysis of reactive trajectories. An important conclusion from the present work is that our results clearly highlight the limitations of computational models where the flexibility of the environment is dramatically reduced by fixing, for example, the position of some atoms of the residues appearing at the active site. Furthermore, a hypothetical success of the frozen-environment approach in reproducing a transmission coefficient, which is clearly not the case for FDH as discussed above, would never imply that the environment could be viewed as static

during the whole reaction process, because the participation of the environment motions in the reaction coordinate can be different at different stages of the reaction progress.

Acknowledgements

We thank the Spanish Ministry Ministerio de Ciencia e Innovación for project CTQ2009-14541-C02, Universitat Jaume I—BANCAIXA Foundation for projects P1·1B2008-36, P1·1B2008-37, and P1·1B2008-38, and Generalitat Valenciana for Prometeo/2009/053. The authors also acknowledge the Servei d'Informatica, Universitat Jaume I for generous allotment of computer time. V. Moliner would like to thank the Spanish Ministerio de Educación for travel financial support, project PR2009-0539. M. Roca thanks the Spanish Ministerio de Ciencia e Innovación for the "Juan de la Cierva" contract.

[1] S. J. Benkovic, G. G. Hammes, S. Hammes-Schiffer, *Biochemistry* **2008**, *47*, 3317–3321.
[2] M. H. M. Olsson, W. W. Parson, A. Warshel, *Chem. Rev.* **2006**, *106*, 1737–1756.
[3] A. R. Clarke, D. B. Wigley, W. N. Chia, D. Barstow, T. Atkinson, J. J. Holbrook, *Nature* **1986**, *324*, 699–702.
[4] J. R. O'Brien, D. J. Schuller, V. S. Yang, B. D. Dillard, W. N. Lanzilotta, *Biochemistry* **2003**, *42*, 5547–5554.
[5] S. C. Kou, B. J. Cherayil, W. Min, B. P. English, X. S. Xie, *J. Phys. Chem. B* **2005**, *109*, 19068–19081.
[6] R. D. Smiley, G. G. Hammes, *Chem. Rev.* **2006**, *106*, 3080–3094.
[7] H. P. Lu, L. Y. Xun, X. S. Xie, *Science* **1998**, *282*, 1877–1882.
[8] H. Yang, G. B. Luo, P. Karnchanaphanurach, T. M. Louie, I. Rech, S. Cova, L. Y. Xun, X. S. Xie, *Science* **2003**, *302*, 262–266.
[9] I. F. Thorpe, C. L. Brooks, *J. Am. Chem. Soc.* **2005**, *127*, 12997–13006.
[10] S. Ferrer, I. Tuñón, S. Martí, V. Moliner, M. Garcia-Viloca, A. González-Lafont, J. M. Lluch, *J. Am. Chem. Soc.* **2006**, *128*, 16851–16863.
[11] S. J. Benkovic, S. Hammes-Schiffer, *Science* **2003**, *301*, 1196–1202.
[12] S. J. Benkovic, S. Hammes-Schiffer, *Science* **2006**, *312*, 208–209.
[13] E. Z. Eisenmesser, O. Millet, W. Labeikovsky, D. M. Korzhnev, M. Wolf-Watz, D. A. Bosco, J. J. Skalicky, L. E. Kay, D. Kern, *Nature* **2005**, *438*, 117–121.
[14] D. D. Boehr, D. McElheny, H. J. Dyson, P. E. Wright, *Science* **2006**, *313*, 1638–1642.
[15] K. A. Henzler-Wildman, V. Thai, M. Lei, M. Ott, M. Wolf-Watz, T. Fenn, E. Pozharski, M. A. Wilson, G. A. Petsko, M. Karplus, C. G. Hubner, D. Kern, *Nature* **2007**, *450*, 838–844.
[16] K. A. Henzler-Wildman, M. Lei, V. Thai, S. J. Kerns, M. Karplus, D. Kern, *Nature* **2007**, *450*, 913–916.
[17] S. Saen-oon, S. Quaytman-Machleder, V. L. Schramm, S. D. Schwartz, *Proc. Natl. Acad. Sci. USA* **2008**, *105*, 16543–16548.
[18] S. Hay, M. J. Sutcliffe, N. S. Scrutton, *Proc. Natl. Acad. Sci. USA* **2007**, *104*, 507–512.
[19] Z. D. Nagel, J. P. Klinman, *Nat. Chem. Biol.* **2009**, *5*, 543–550.
[20] A. V. Pisliakov, J. Cao, S. C. L. Kamerlin, A. Warshel, *Proc. Natl. Acad. Sci. USA* **2009**, *106*, 17359–17364.
[21] M. Roca, V. Moliner, I. Tuñón, J. T. Hynes, *J. Am. Chem. Soc.* **2006**, *128*, 6186–6193.
[22] R. Castillo, M. Roca, A. Soriano, V. Moliner, I. Tuñón, *J. Phys. Chem. B* **2007**, *111*, 529–534.
[23] J. J. Ruiz-Pernía, I. Tuñón, V. Moliner, J. T. Hynes, M. Roca, *J. Am. Chem. Soc.* **2008**, *130*, 7477–7488.
[24] S. Glasstone, K. J. Laidler, H. Eyring, *The Theory of Rate Processes*, McGraw-Hill, New York, **1941**.
[25] J. C. Keck, *Adv. Chem. Phys.* **1967**, *13*, 85–121.
[26] D. G. Truhlar, B. C. Garrett, S. J. Klippenstein, *J. Phys. Chem.* **1996**, *100*, 12771–12800.
[27] H. J. Kim, J. T. Hynes, *J. Am. Chem. Soc.* **1992**, *114*, 10508–10528.
[28] R. F. Grote, J. T. Hynes, *J. Chem. Phys.* **1980**, *73*, 2715–2732.
[29] J. T. Hynes, M. Baer, *The Theory of Chemical Reaction Dynamics*, CRC Press, Boca Raton, **1985**.
[30] V. I. Tishkov, V. O. Popov, *Biomol. Eng.* **2006**, *23*, 89–110.
[31] R. Wichmann, C. Wandrey, A. F. Buckmann, M. R. Kula, *Biotechnol. Bioeng.* **2000**, *67*, 791–804.
[32] G. Krix, A. S. Bommarius, K. Drauz, M. Kottenhahn, M. Schwarm, M. R. Kula, *J. Biotechnol.* **1997**, *53*, 29–39.
[33] A. M. Rojkova, A. G. Galkin, L. B. Kulakova, A. E. Serov, P. A. Savitsky, V. V. Fedorchuk, V. I. Tishkov, *FEBS Lett.* **1999**, *445*, 183–188.
[34] H. Xue, X. W. Wu, W. P. Huskey, *J. Am. Chem. Soc.* **1996**, *118*, 5804–5805.
[35] J. S. Blanchard, W. W. Cleland, *Biochemistry* **1980**, *19*, 3543–3550.
[36] J. D. Hermes, S. W. Morrical, M. H. O'Leary, W. W. Cleland, *Biochemistry* **1984**, *23*, 5479–5488.
[37] V. I. Tishkov, A. G. Galkin, A. M. Yegorov, *Dokl. Akad. Nauk SSSR* **1991**, *317*, 745–748.
[38] M. Iida, K. Kitamura-Kimura, H. Maeda, S. Mineki, *Biosci. Biotechnol. Biochem.* **1992**, *56*, 1966–1970.
[39] B. Schiøtt, Y. J. Zheng, T. C. Bruice, *J. Am. Chem. Soc.* **1998**, *120*, 7192–7200.
[40] J. N. Bandaria, C. M. Cheatum, A. Kohen, *J. Am. Chem. Soc.* **2009**, *131*, 10151–10155.
[41] V. I. Tishkov, A. D. Matorin, A. M. Rojkova, V. V. Fedorchuk, P. A. Savitsky, L. A. Dementieva, V. S. Lamzin, A. V. Mezentzev, V. O. Popov, *FEBS Lett.* **1996**, *390*, 104–108.
[42] V. S. Lamzin, Z. Dauter, V. O. Popov, E. H. Harutyunyan, K. S. Wilson, *J. Mol. Biol.* **1994**, *236*, 759–785.
[43] A. G. Galkin, A. S. Kutsenko, N. P. Bajulina, N. G. Esipova, V. S. Lamzin, A. V. Mesentsev, D. V. Shelukho, T. V. Tikhonova, V. I. Tishkov, T. B. Ustinnikova, V. O. Popov, *Biochim. Biophys. Acta Protein Struct. Mol. Enzymol.* **2002**, *1594*, 136–149.
[44] I. G. Shabalin, E. V. Filippova, K. M. Polyakov, E. G. Sadykhov, T. N. Safonova, T. V. Tikhonova, V. I. Tishkov, V. O. Popov, *Acta Crystallogr. Sect. A* **2009**, *65*, 1315–1325.
[45] R. Castillo, M. Oliva, S. Martí, V. Moliner, *J. Phys. Chem. B* **2008**, *112*, 10012–10022.
[46] M. J. S. Dewar, E. G. Zoebisch, E. F. Healy, J. J. P. Stewart, *J. Am. Chem. Soc.* **1985**, *107*, 3902–3909.
[47] W. L. Jorgensen, J. Tirado-Rives, *J. Am. Chem. Soc.* **1988**, *110*, 1657–1666.
[48] G. A. Kaminski, R. A. Friesner, J. Tirado-Rives, W. L. Jorgensen, *J. Phys. Chem. B* **2001**, *105*, 6474–6487.
[49] W. L. Jorgensen, J. Chandrasekhar, J. D. Madura, R. W. Impey, M. L. Klein, *J. Chem. Phys.* **1983**, *79*, 926–935.
[50] M. J. Field, M. Albe, C. Bret, F. Proust-De Martin, A. Thomas, *J. Comput. Chem.* **2000**, *21*, 1088–1100.
[51] M. J. Field, P. A. Bash, M. Karplus, *J. Comput. Chem.* **1990**, *11*, 700–733.
[52] A. Warshel, M. Levitt, *J. Mol. Biol.* **1976**, *103*, 227–249.
[53] L. Verlet, *Phys. Rev.* **1967**, *159*, 98.
[54] W. C. Swope, H. C. Andersen, P. H. Berens, K. R. Wilson, *J. Chem. Phys.* **1982**, *76*, 637–649.
[55] S. Kumar, D. Bouzida, R. H. Swendsen, P. A. Kollman, J. M. Rosenberg, *J. Comput. Chem.* **1992**, *13*, 1011–1021.
[56] G. M. Torrie, J. P. Valleau, *J. Comput. Phys.* **1977**, *23*, 187–199.
[57] K. Nam, X. Prat-Resina, M. Garcia-Viloca, L. S. Devi-Kesavan, J. Gao, *J. Am. Chem. Soc.* **2004**, *126*, 1369–1376.
[58] M. P. Allen, D. J. Tildesley, *Computer Simulations of Liquids*, Oxford, Clarendon, **1989**.
[59] J. P. Bergsma, B. J. Gertner, K. R. Wilson, J. T. Hynes, *J. Chem. Phys.* **1987**, *86*, 1356–1376.
[60] B. J. Gertner, K. R. Wilson, J. T. Hynes, *J. Chem. Phys.* **1989**, *90*, 3537–3558.
[61] H. C. Andersen, *J. Comput. Phys.* **1983**, *52*, 24–34.
[62] B. J. Gertner, R. M. Whitnell, K. R. Wilson, J. T. Hynes, *J. Am. Chem. Soc.* **1991**, *113*, 74–87.
[63] S. Hammes-Schiffer, *Biochemistry* **2002**, *41*, 13335–13343.

[64] H. A. Kramers, *Physica* **1940**, *7*, 284–304.
[65] A. Soriano, E. Silla, I. Tuñón and M. F. Ruiz-López, *J. Am. Chem. Soc.* **2005**, *127*, 1946–1957.
[66] P. K. Agarwal, *J. Am. Chem. Soc.* **2005**, *127*, 15248–15256.
[67] K. G. Brown, S. C. Erfurth, E. W. Small, W. L. Peticolas, *Proc. Natl. Acad. Sci. USA* **1972**, *69*, 1467–1469.
[68] N. Go, T. Noguti, T. Nishikawa, *Proc. Natl. Acad. Sci. USA* **1983**, *80*, 3696–3700.
[69] K. C. Chou, *Biochem. J.* **1983**, *215*, 465–469.
[70] V. Moliner, A. J. Turner, I. H. Williams, *Chem. Commun.* **1997**, 1271–1272.
[71] A. J. Turner, V. Moliner, I. H. Williams, *Phys. Chem. Chem. Phys.* **1999**, *1*, 1323–1331.
[72] S. Martí, V. Moliner, I. Tuñón, *J. Chem. Theory Comput.* **2005**, *1*, 216–216.

Received: March 11, 2010
Published online: August 16, 2010

